

# Dynamical Density-Matrix Renormalization for Single Impurity Anderson Models

Carsten Raas

Michał Karski

Götz S. Uhrig

*Institute for Theoretical Physics  
University of Cologne*

Collaborations:  
Frithjof B. Anders (*Bremen*)

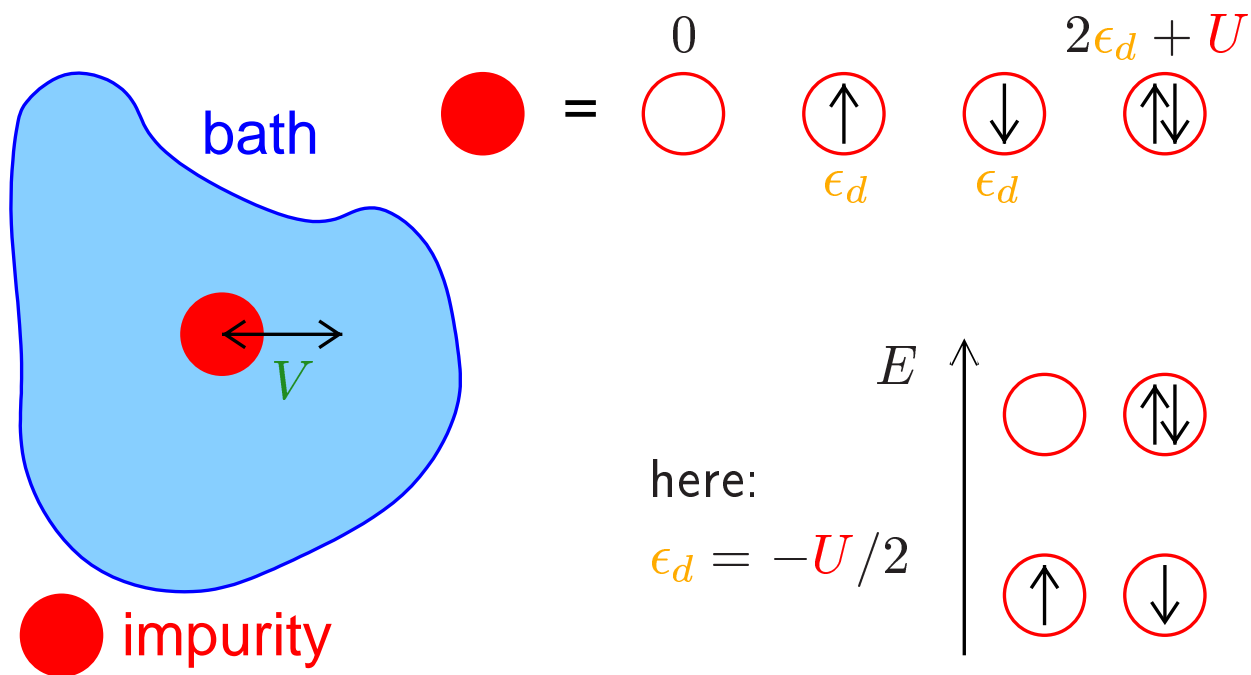
Leiden - 2004/8/3

# Overview

- Single impurity Anderson model (SIAM)
- Dynamical density-matrix renormalization
  - Correction vector D-DMRG
  - Technical details
  - Deconvolution strategies
- Dynamics of the SIAM
  - Hubbard satellites
  - Kondo energy scale
- Dynamical mean-field theory (DMFT)
  - $d = \infty$  (Bethe lattice) Hubbard model
  - Metallic and insulating solutions
  - Mott-Hubbard transition
- Outlook

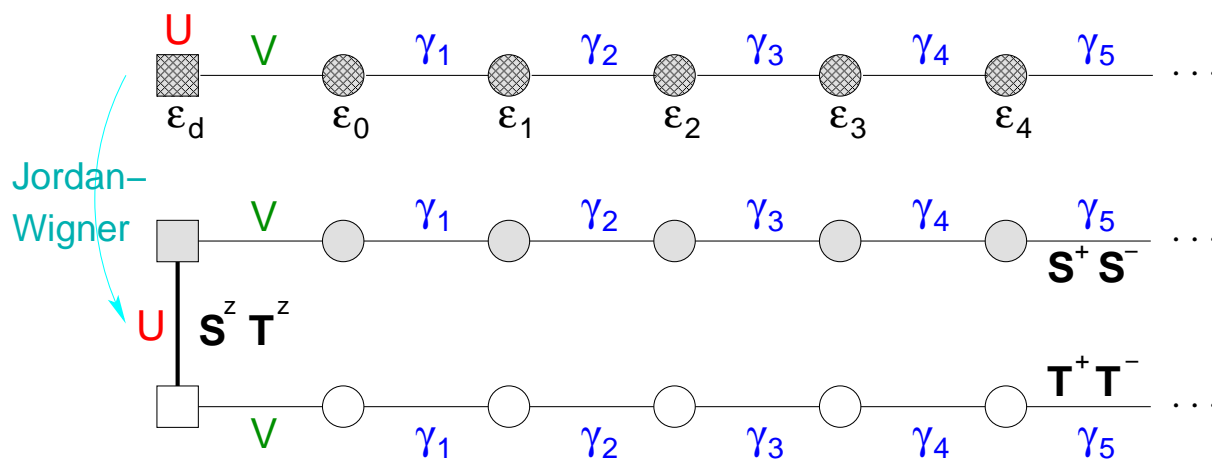
# Single impurity Anderson model I

$$\mathcal{H} = \sum_{\sigma} \epsilon_d n_{d,\sigma} + U n_{d,\downarrow} n_{d,\uparrow} + \sum_{\sigma} \left( V d_{\sigma}^{\dagger} c_{1,\sigma} + \text{h.c.} \right) + \sum_{\sigma,j} \epsilon_j c_{j,\sigma}^{\dagger} c_{j,\sigma} + \sum_{\sigma,j} \left( \gamma_j c_{j,\sigma}^{\dagger} c_{j+1,\sigma} + \text{h.c.} \right)$$

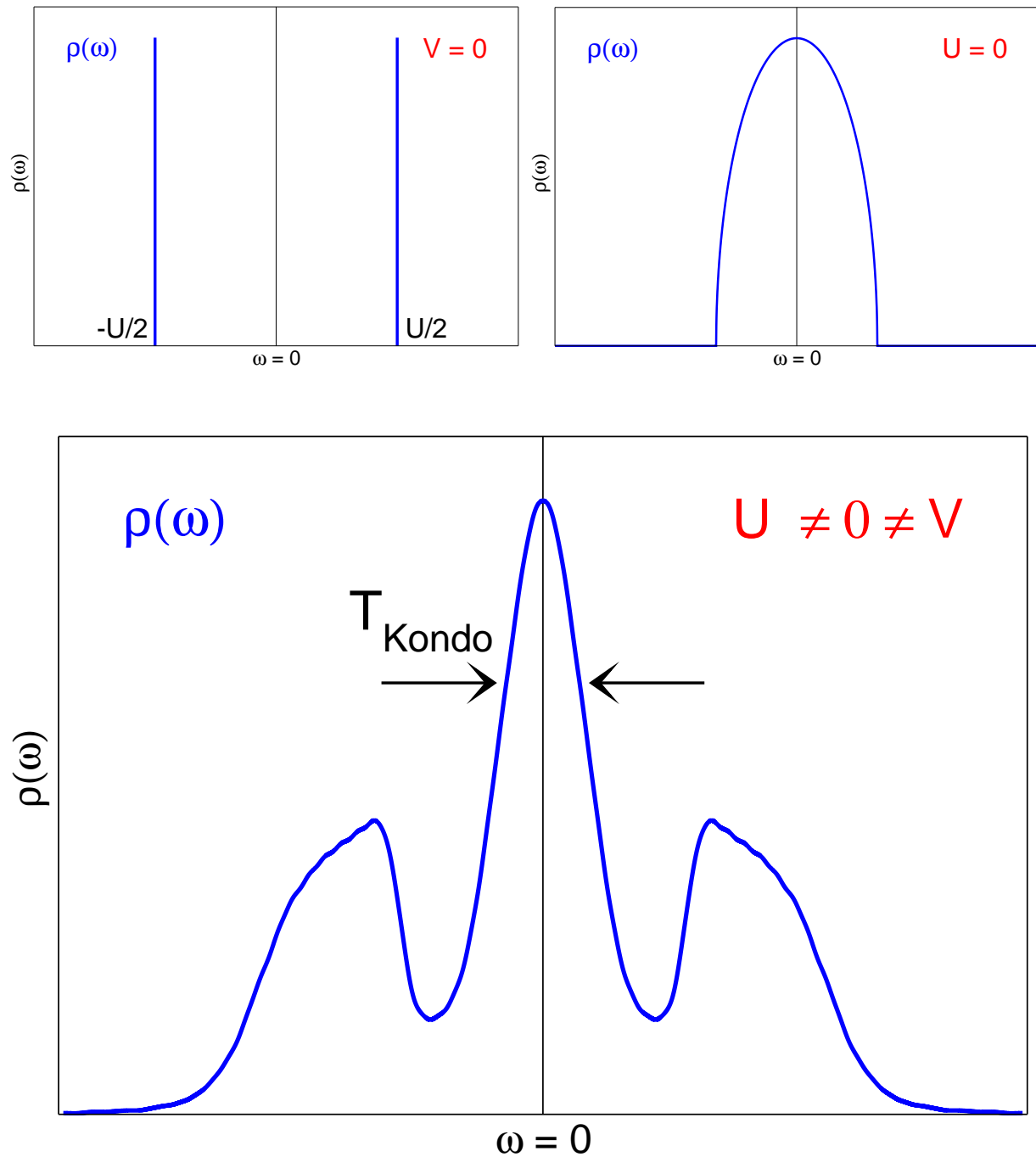


Map  $\{\uparrow\downarrow\}, \{\uparrow -\}, \{-\downarrow\}, \{- -\}$  onto

$$\downarrow = \begin{cases} \text{occupied} \Rightarrow \mathbf{S} \uparrow \\ \text{empty} \Rightarrow \mathbf{S} \downarrow \end{cases} \quad \uparrow = \begin{cases} \text{occupied} \Rightarrow \mathbf{T} \uparrow \\ \text{empty} \Rightarrow \mathbf{T} \downarrow \end{cases}$$



# Single impurity Anderson model II



- Kondo energy scale  $T_{\text{Kondo}}$  exponentially small
- $\rho(\omega = 0)$  remains untouched by the interaction  $U$

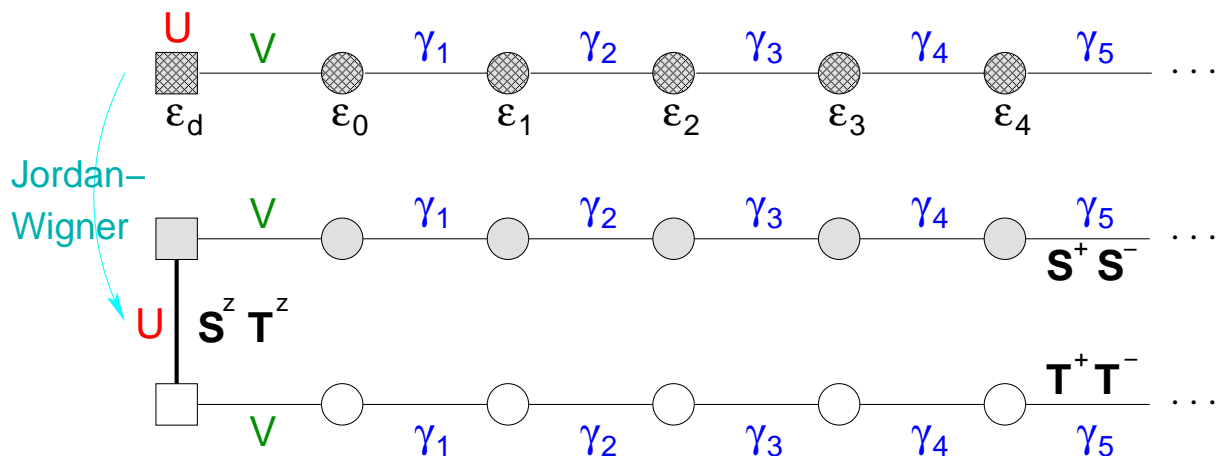
# Single impurity Anderson model III

$$\begin{aligned}
 \mathcal{H} = & \epsilon_d + U/4 + \sum_{j>0} \epsilon_j + (\epsilon_d + U/2) (\mathbf{S}_0^z + \mathbf{T}_0^z) \\
 & + \sum_{j>0} \epsilon_j (\mathbf{S}_j^z + \mathbf{T}_j^z) + U \mathbf{S}_0^z \mathbf{T}_0^z \\
 & + \sum_j [\gamma_j (\mathbf{S}_j^+ \mathbf{S}_{j+1}^- + \mathbf{T}_j^+ \mathbf{T}_{j+1}^-) + \text{h.c.}]
 \end{aligned}$$

$$(\gamma_0 := V)$$

$$\begin{aligned}
 \epsilon_d = -U/2 \quad \text{and} \quad \epsilon_j = 0 \quad \forall j>0 \\
 \Rightarrow \quad \text{particle-hole symmetric}
 \end{aligned}$$

$$\begin{aligned}
 \mathcal{H} = & -U/4 + U \mathbf{S}_0^z \mathbf{T}_0^z \\
 & + \sum_j [\gamma_j (\mathbf{S}_j^+ \mathbf{S}_{j+1}^- + \mathbf{T}_j^+ \mathbf{T}_{j+1}^-) + \text{h.c.}]
 \end{aligned}$$



# Dynamical DMRG

## Correction vector Density-Matrix Renormalization

→ T.D. Kühner and S.R. White, Phys. Rev. B **60**, 335 (1999)

$$z := \omega + i\eta$$

$$G^>(z) = \langle \Psi_0 | \mathbf{S}_0^- \underbrace{\frac{1}{z - (\mathcal{H} - E_0)}}_{|\mathbf{cv}\rangle} \mathbf{S}_0^+ | \Psi_0 \rangle$$

particle-hole symmetric:  $G(z) = G^>(z) - G^>(-z)$

$$\text{Calculate CV: } \underbrace{[\omega + i\eta - (\mathcal{H} - E_0)]}_{\mathbf{A}} |\mathbf{cv}\rangle = \mathbf{S}_0^+ | \Psi_0 \rangle$$

- inversion of an almost singular non-Hermitian matrix  $\mathbf{A}$

but:  $\mathbf{A} = \mathbf{A}^T$  is complex symmetric.

- symmetry not used when

$$[\underbrace{((\mathcal{H} - E_0) - \omega)^2 + \eta^2}_{\mathfrak{S}}] |\mathfrak{S}\mathbf{cv}\rangle = -\eta \mathbf{S}_0^+ | \Psi_0 \rangle$$

$$|\mathfrak{R}\mathbf{cv}\rangle = \frac{1}{\eta} [\omega - (\mathcal{H} - E_0)] |\mathfrak{S}\mathbf{cv}\rangle$$

- ▶ prefer the full complex system (linear in  $\mathcal{H}$ )

DMRG target states:  $\mathbf{S}_0^+ \begin{array}{l} | \Psi_0 \rangle \\ | \Psi_0 \rangle \end{array} \begin{array}{l} 40\% \\ 20\% \end{array} \left| \begin{array}{l} | \mathfrak{S}\mathbf{cv} \rangle \\ | \mathfrak{R}\mathbf{cv} \rangle \end{array} \begin{array}{l} 20\% \\ 20\% \end{array} \right.$

# Performance of iterative solvers

- CG (conjugate gradients)

→ M.R. Hestenes, E. Stiefel, NBS J. Res., **49** 409-436 (1952)

- BiCGSTAB

→ H.A. van der Vorst, SIAM J. Sci. Stat. Comput. **13** 631-644 (1992)

- Complex Symmetric QMR (quasi-minimal residual)

→ R.W. Freund, SIAM J. Sci. Comput. **14**(2) 470-482 (1993)

+ Preconditioning (PC):  $\mathbf{Ax} = \mathbf{b} \rightarrow \underbrace{\mathbf{PA}}_{\tilde{\mathbf{A}}} \mathbf{x} = \underbrace{\mathbf{Pb}}_{\tilde{\mathbf{b}}}$

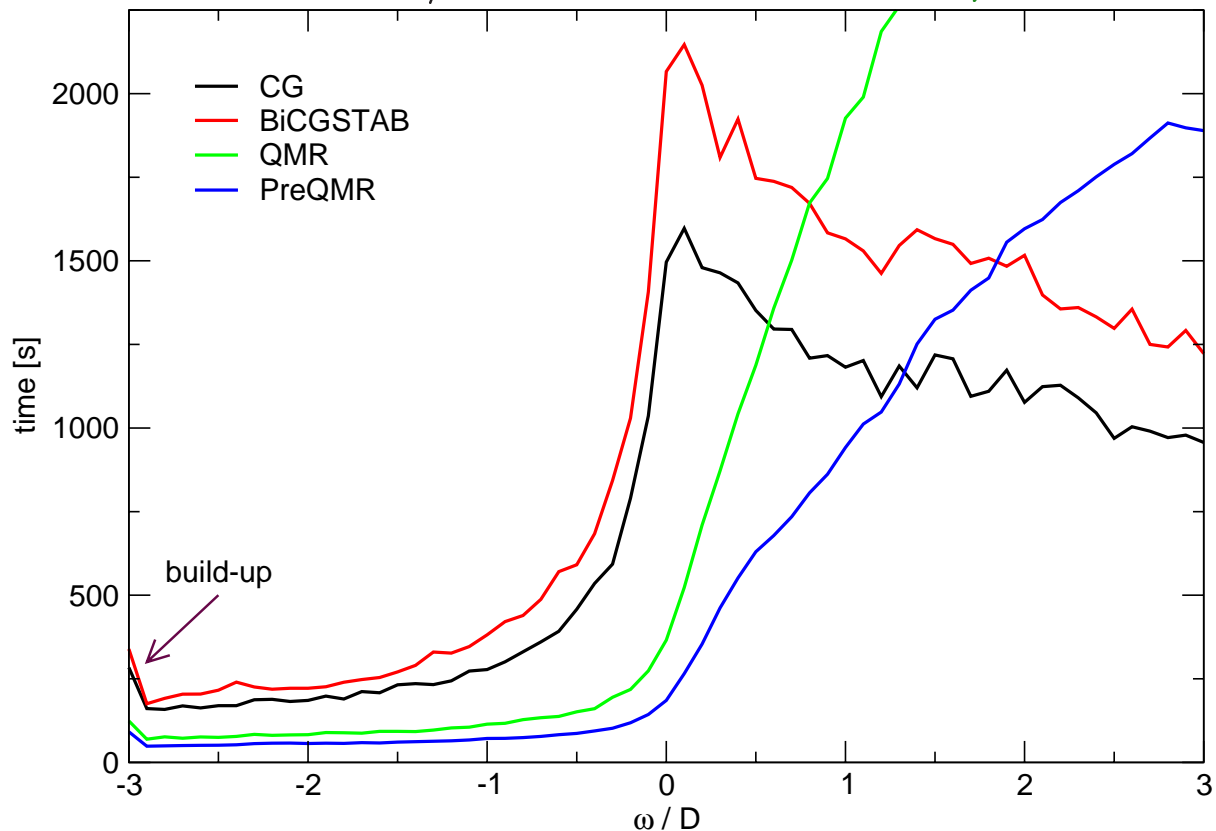
- Standard method: Incomplete LU factorization (ILU)

- DMRG-inspired preconditioner:

▶ Diagonalize  $\mathcal{H}_S$  and  $\mathcal{H}_E \rightarrow \mathcal{H}_S^{-1}$  and  $\mathcal{H}_E^{-1}$

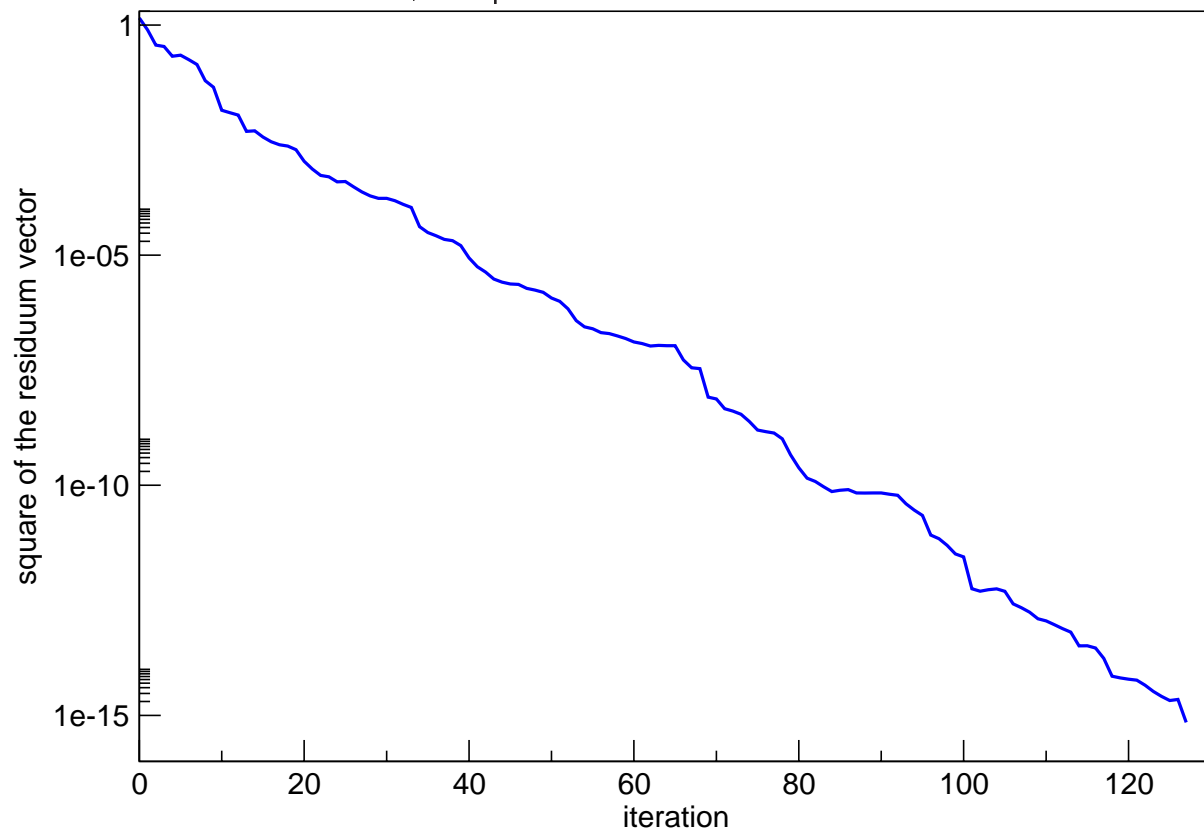
▶ Pseudo-inverse of  $\mathbf{A}$  without  $\mathcal{H}_{S-E}$

$U = 2D$ ,  $V = D/2$ ,  $L_f = 120$ ,  $m = 128$ ,  $\eta = 0.1D$



# QMR convergence

$U = 2D$ ,  $V = D/2$ ,  $L_f = 120$ ,  $m = 128$ ,  $\omega = 1D$ ,  $\eta = 0.1D$



# Evaluate the Green's function

$$-\pi\rho^{(\eta)}(\omega) = \Im \langle \Psi_0 | \mathcal{R}^\dagger \underbrace{\frac{1}{\omega + i\eta - \Delta\mathcal{H}}}_{|\mathbf{cv}\rangle} \mathcal{R} | \Psi_0 \rangle$$

$$\Delta\mathcal{H} = \mathcal{H} - E_0$$

Three methods:

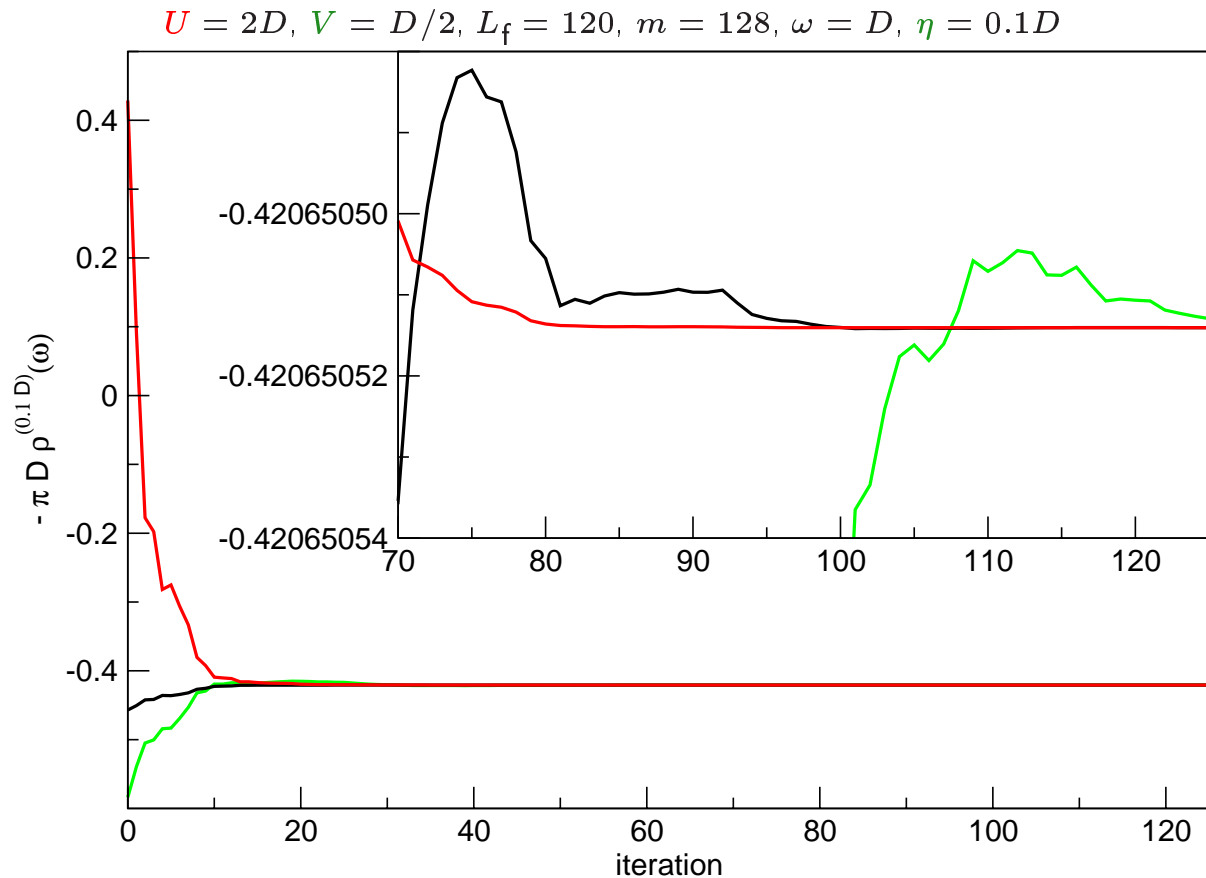
**#1**  $-\pi\rho = \langle \Psi_0 | \mathcal{R}^\dagger | \mathfrak{S} \mathbf{cv} \rangle$

→ T.D. Kühner and S.R. White, Phys. Rev. B **60**, 335 (1999)

**#2**  $-\pi\rho = \frac{1}{\eta} [\langle \mathfrak{S} \mathbf{cv} | (\omega - \Delta\mathcal{H})^2 + \eta^2 | \mathfrak{S} \mathbf{cv} \rangle + \eta \langle \mathfrak{S} \mathbf{cv} | \mathcal{R} | \Psi_0 \rangle + \eta \langle \Psi_0 | \mathcal{R}^\dagger | \mathfrak{S} \mathbf{cv} \rangle]$

→ E. Jeckelmann, Phys. Rev. B **66**, 045114 (2002)

**#3**  $-\pi\rho = -\eta \langle \mathbf{cv} | \mathbf{cv} \rangle$

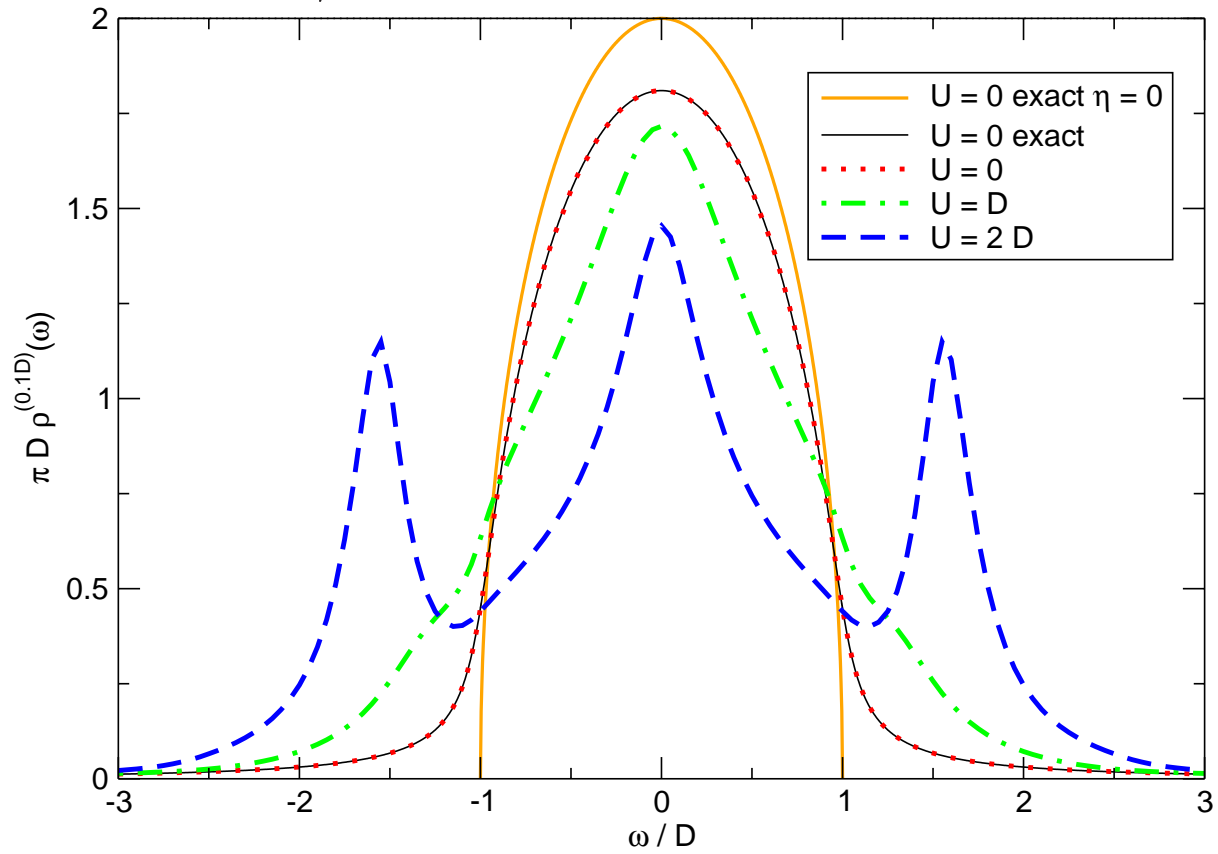


# Results

D-DMRG  $\rho^{(\eta)}(\omega) = -\frac{1}{\pi} \Im G(z)$  convolved

with Lorentzian of width  $\eta$ :  $L_\eta(\omega) = \frac{\eta}{\pi(\omega^2 + \eta^2)}$

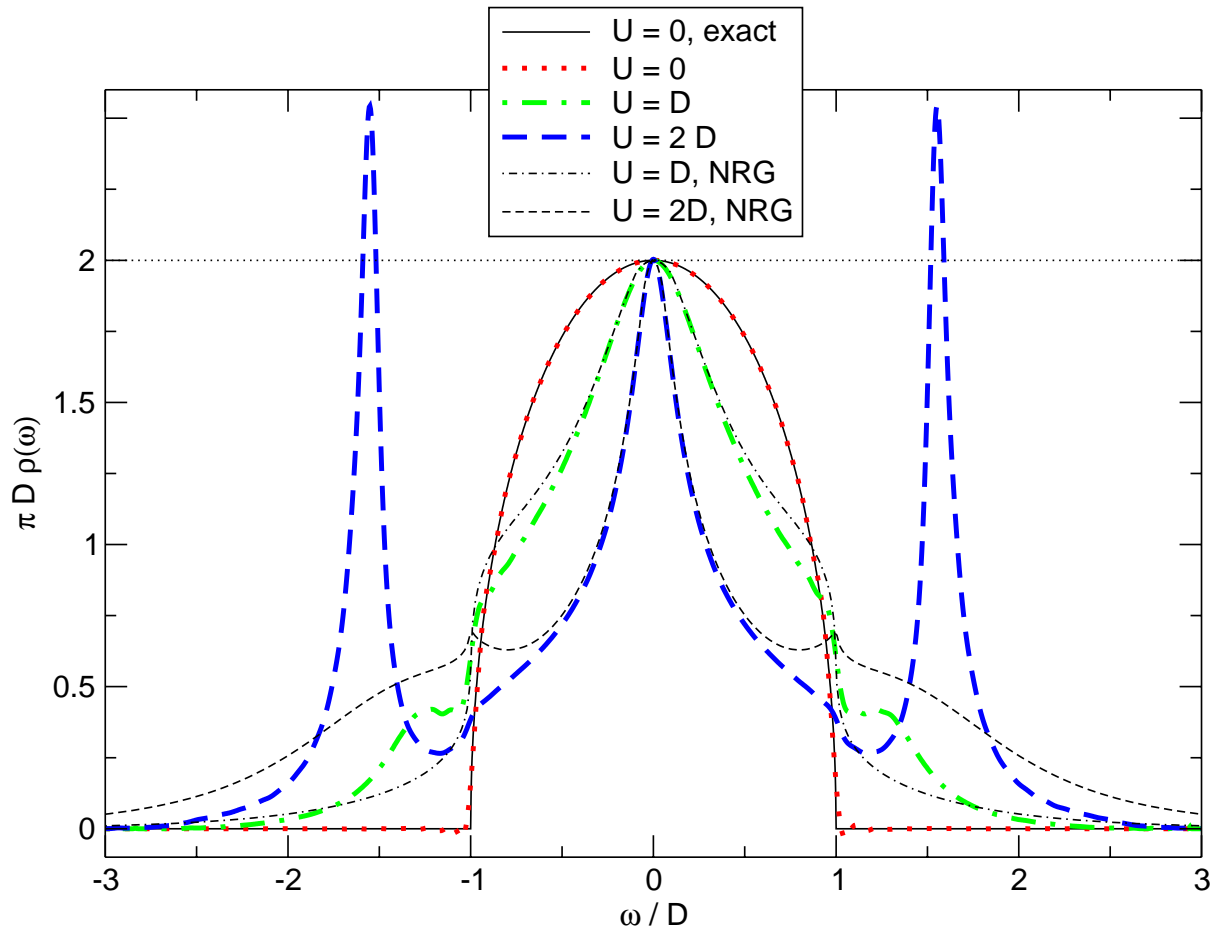
$V = D/2, L_f = 80, m = 128, \eta = 0.1D$



# Deconvolution strategies I

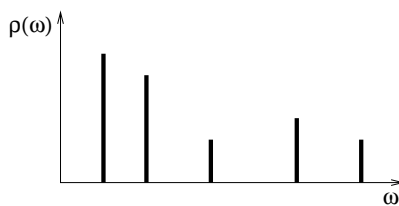
## Linear methods

- Fourier transformation:  
FFT, division by  $\exp(-\eta\tau)$ , low-pass filtering

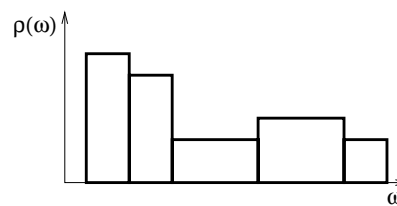


- $\underline{g} = \underline{\underline{M}} \underline{w}$  with  $g_i$ : DMRG data  
 $w_i$ : wanted weights

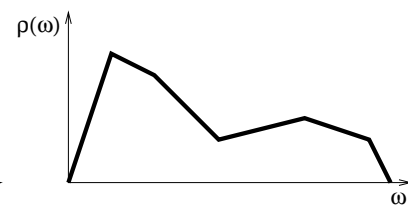
► Direct inversion of  $\underline{\underline{M}}$  by assuming



$\delta$ -functions



bars



piecewise linearity

→ F. Gebhard *et al.*, Eur. Phys. B **36**, 491-509 (2003)

# Deconvolution strategies II

## Least-Bias deconvolution

In contrast to FFT or direct inversion

- non-linear method.

Least-Bias implies maximum entropy.

maximize  $-\int \rho(\omega) \ln(\rho(\omega)) d\omega$

with conditions  $g_i = \int L_{\eta_i}(\omega - \xi_i) \rho(\omega) d\omega$

leads to an ansatz for the spectral density

$$\rho(\omega) = \exp \left[ \sum_i \lambda_i L_{\eta_i}(\omega - \xi_i) \right]$$

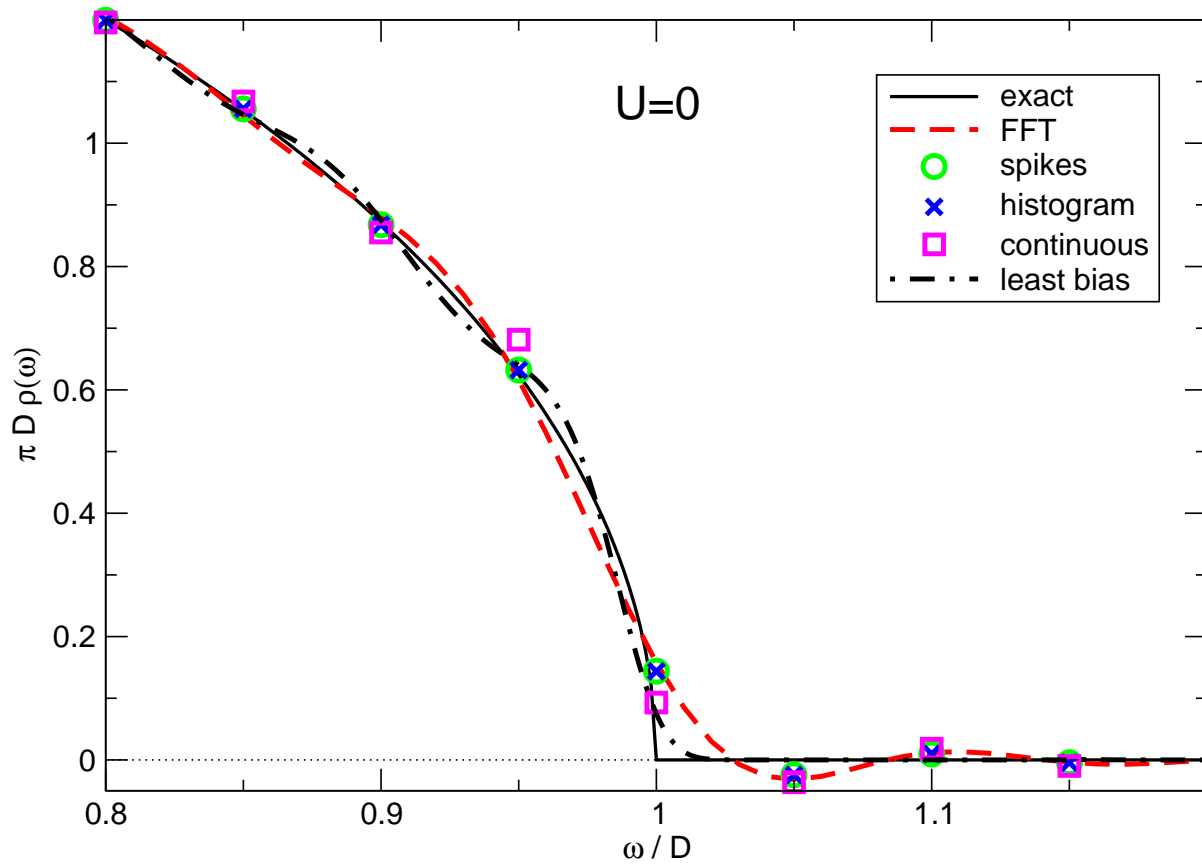
continuous and positive definite

→ CR and G.S. Uhrig, in preparation

$\xi_i$  D-DMRG frequency     $\{\lambda_i\}$  Lagrange multipliers

$g_i$  D-DMRG data at  $\xi_i$      $L_{\eta_i}(\omega) = \frac{\eta_i}{\pi(\omega^2 + \eta_i^2)}$

# Deconvolution: comparison I



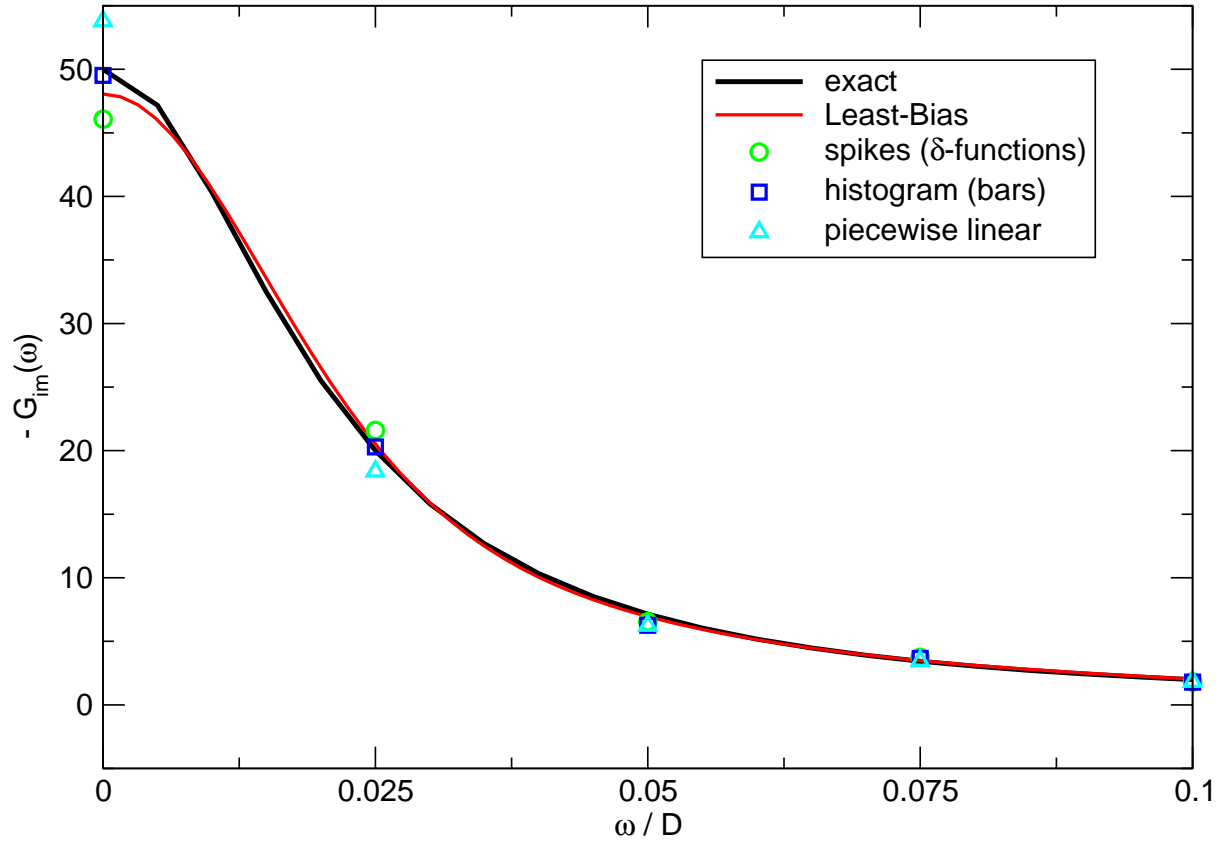
- Least-Bias deconvolution:

- ▶ continuous and positive definite

# Deconvolution: comparison: II

exact  $\Im G(\omega)$ ,  $U = 0$ ,  $V = 0.1D$

$\eta = 0.1D$ ,  $\delta\omega = 0.025D$

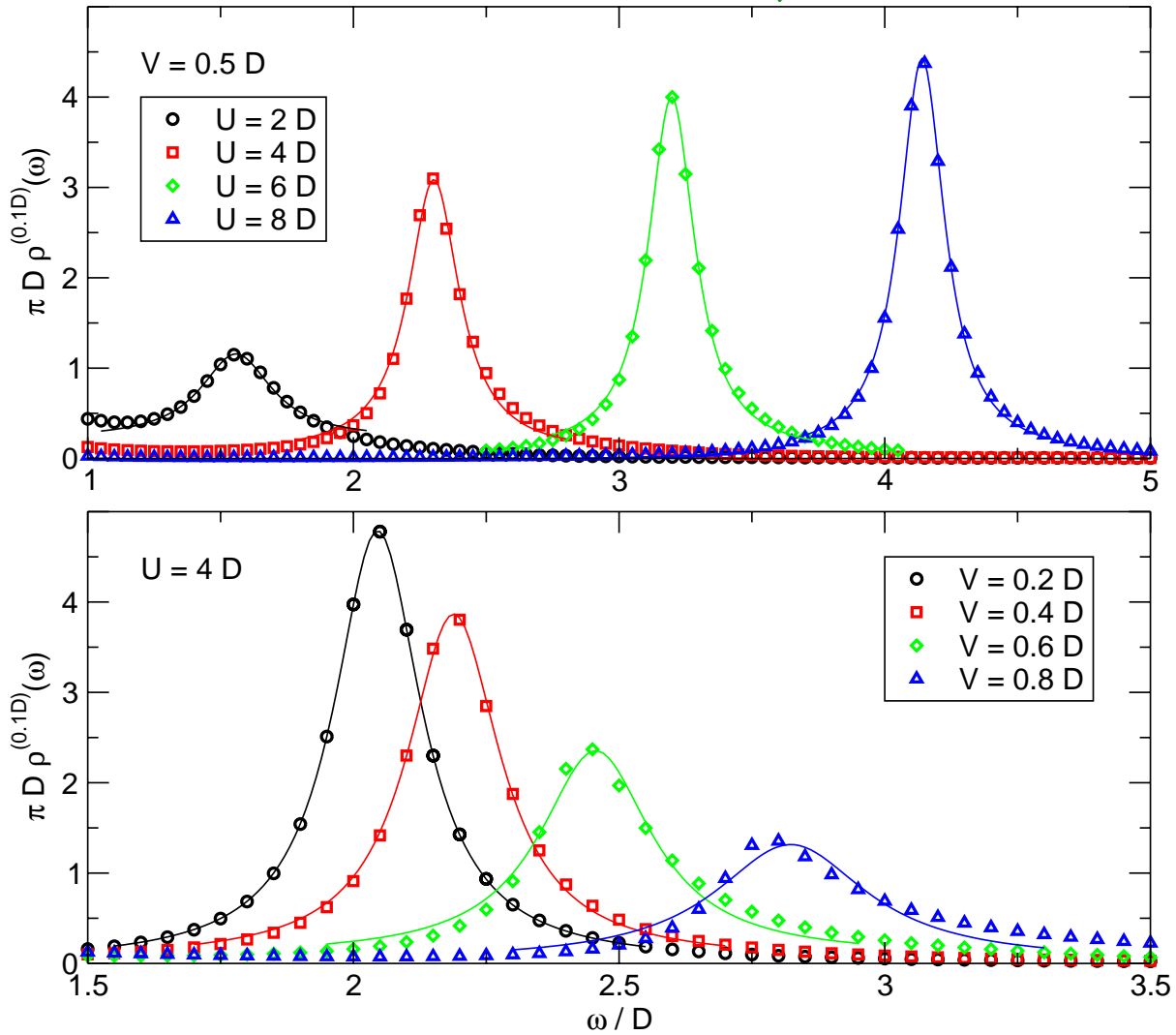


- Least-Bias deconvolution:
  - ▶ continuous and positive definite

# Hubbard satellites I

- Dominant, sharp side band peaks

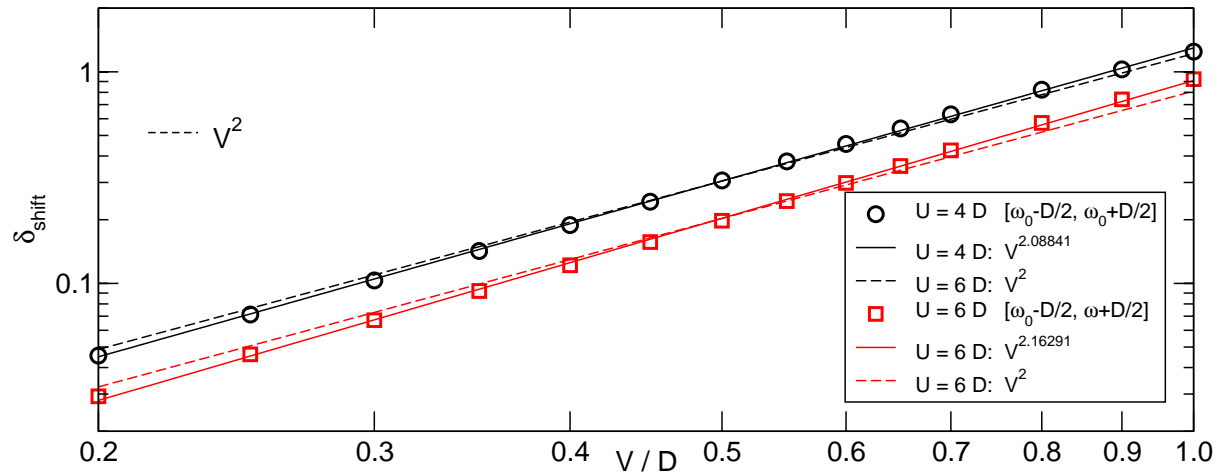
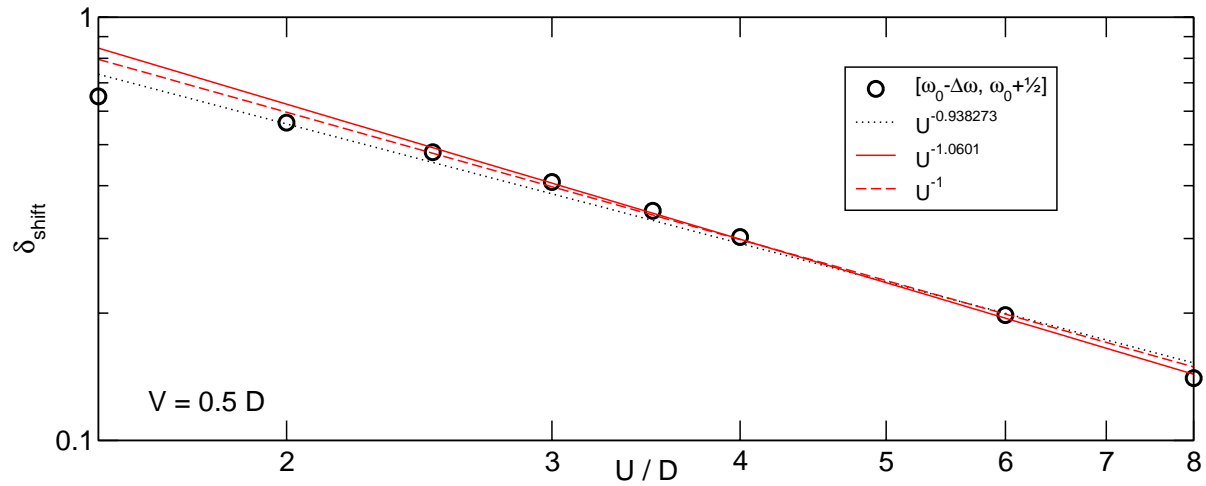
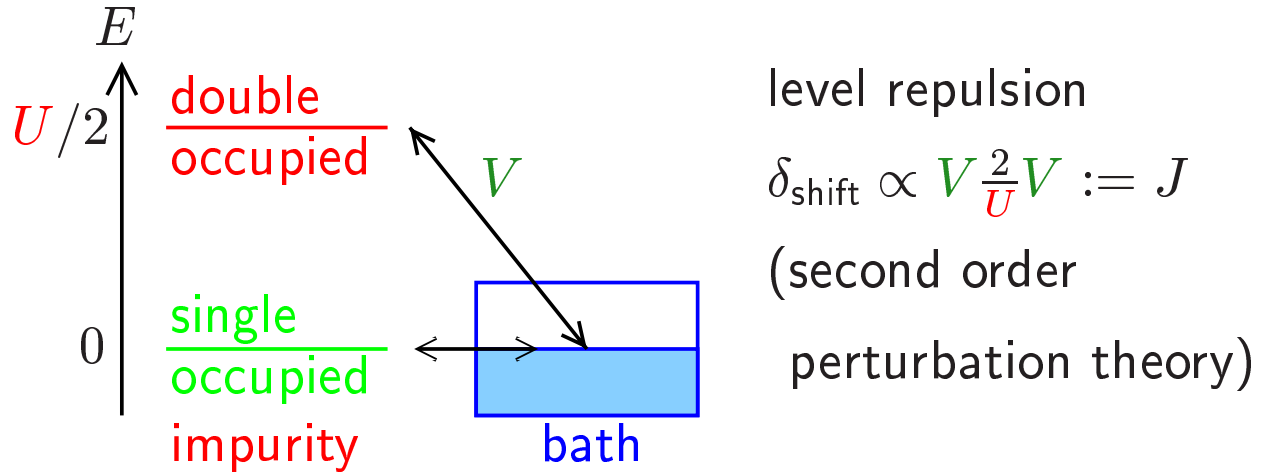
$$L_f = 40 - 80, m = 128, \eta = 0.1D$$



- symbols: D-DMRG data  
lines: Lorentz fit  $L(\eta_{\text{fit}})$
- positions:  $U/2 + \delta_{\text{shift}}$
- width:  $L(\eta_{\text{true}}) \otimes L(\eta) = L(\eta_{\text{true}} + \eta)$   
 $\Rightarrow \eta_{\text{true}} = \eta_{\text{fit}} - \eta$

# Hubbard satellites II: positions

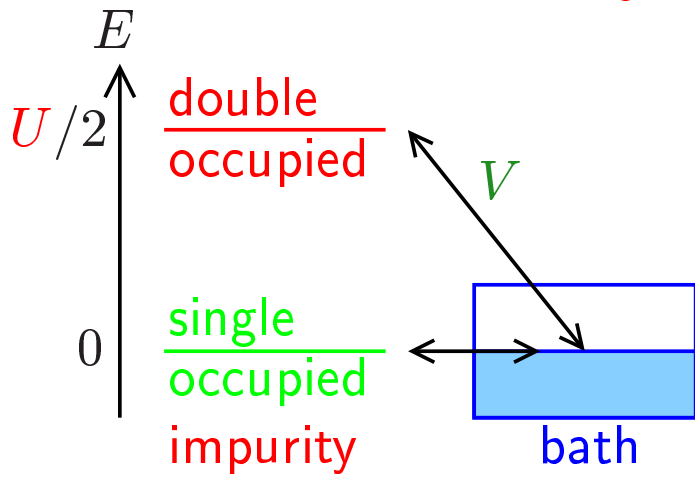
- Shifts of positions:  $\omega_{\pm} = \pm(\frac{U}{2} + \delta_{\text{shift}})$



→ CR, G.S. Uhrig, and F.B. Anders, Phys. Rev. B **69**(4), 041102(R) (2004)

# Hubbard satellites III: width

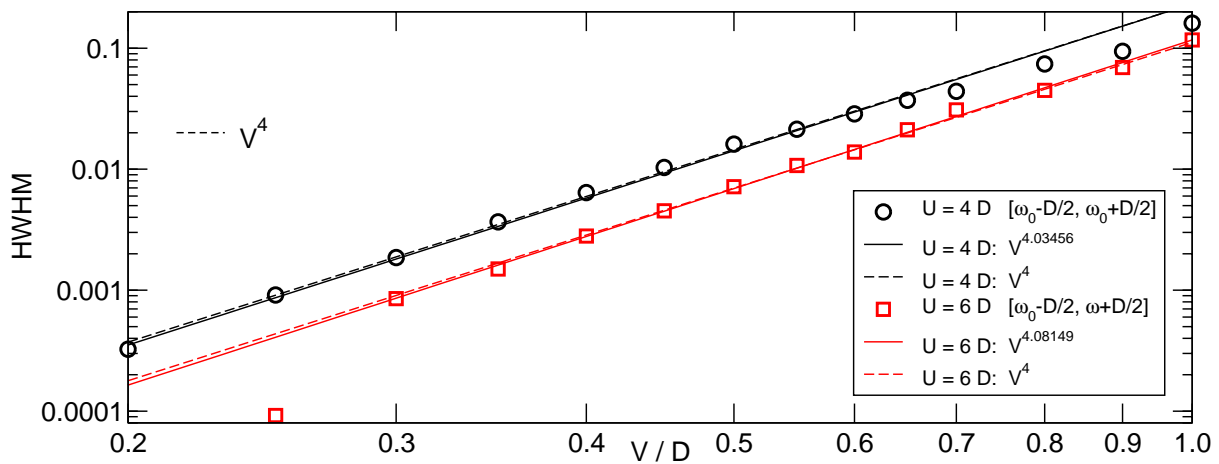
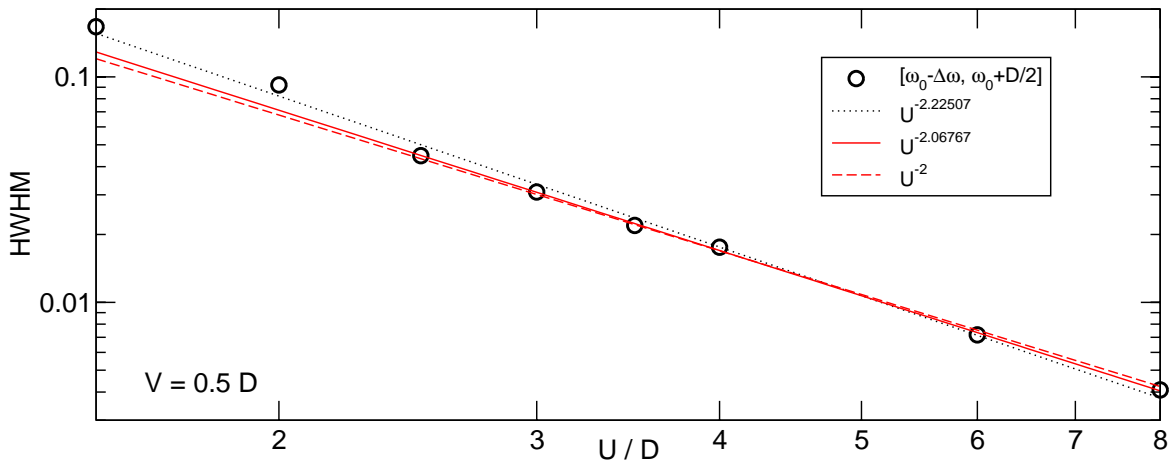
- Line widths:  $\text{HWHM} \propto \frac{V^4}{U^2 D}$



Fermi's golden rule

$$J := V \frac{2}{U} V$$

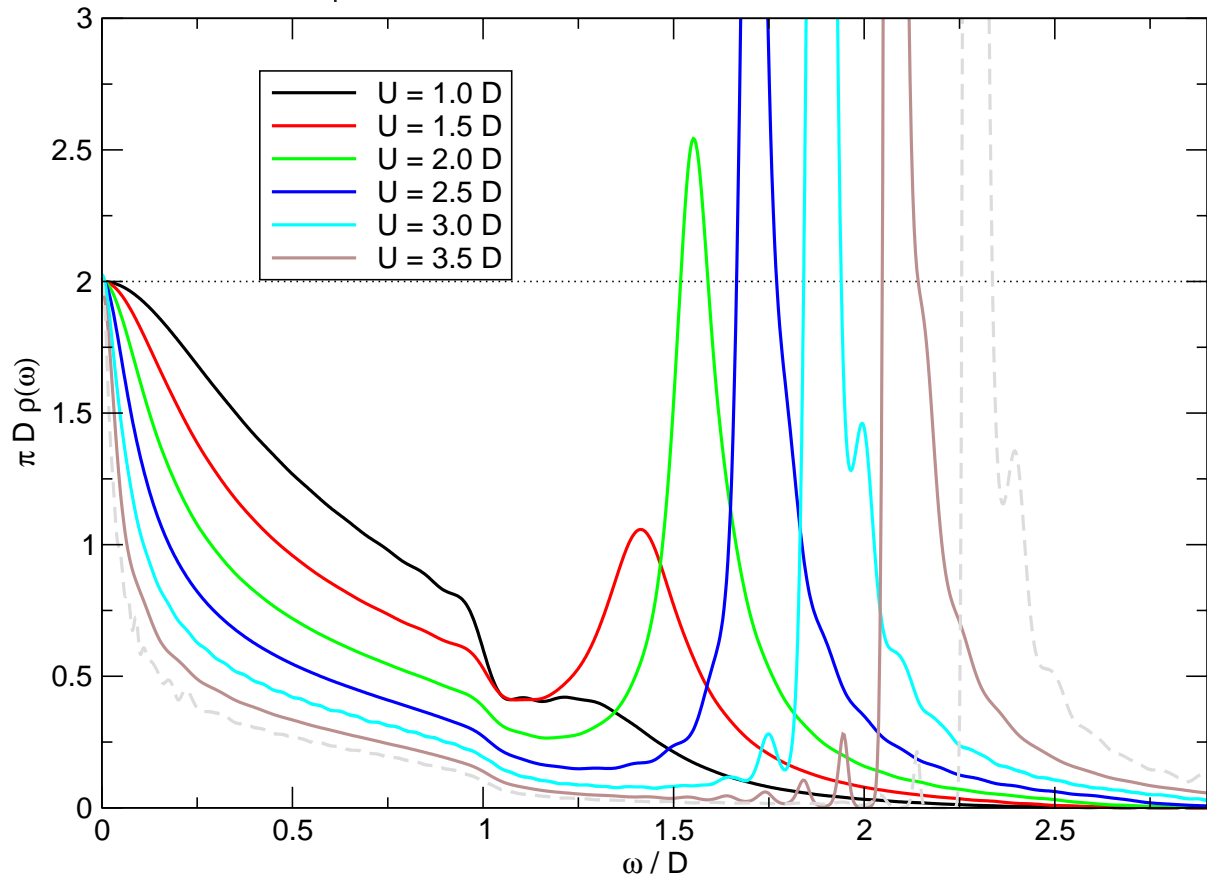
$$\eta_{\text{true}} \propto \frac{J^2}{D} \propto \frac{V^4}{U^2 D}$$



→ CR, G.S. Uhrig, and F.B. Anders, Phys. Rev. B **69**(4), 041102(R) (2004)

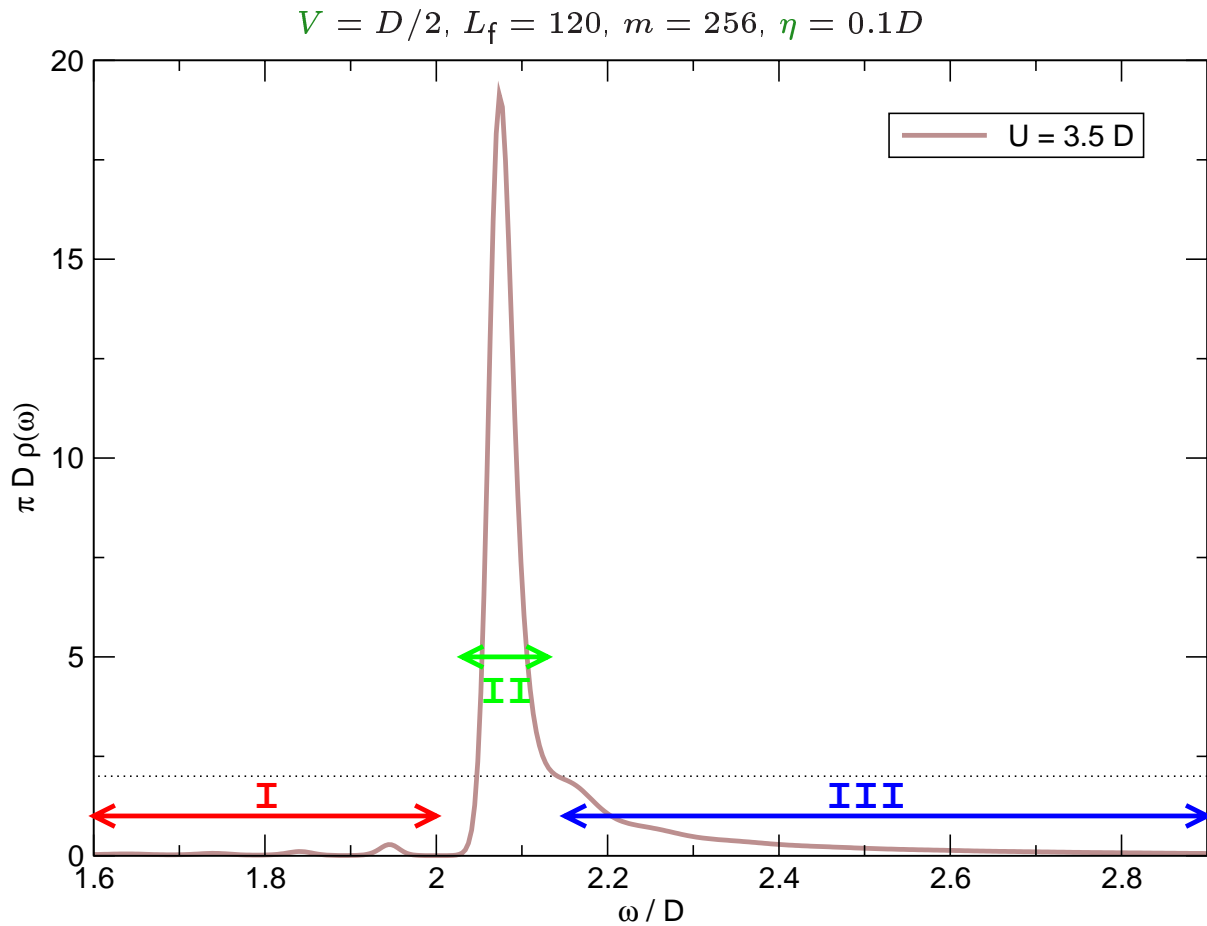
# Hubbard satellites IVa: lineshape

$V = D/2, L_f = 120 - 400, m = 128 - 256, \eta = 0.1 - 0.01D$



► asymmetric satellite with tail towards high energies

# Hubbard satellites IVb: lineshape



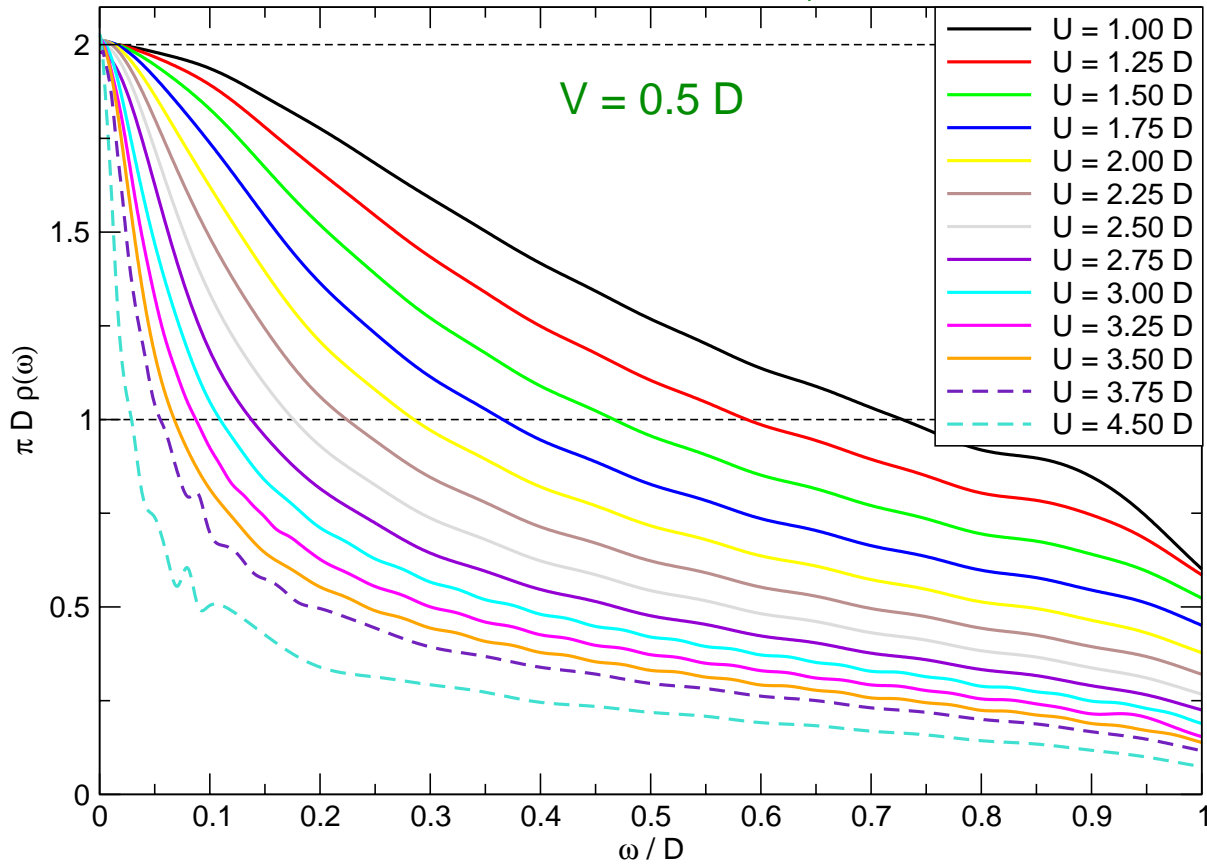
**I** decaying weight of the free band

**II** weakly broadened impurity level;  
double occupancy decays into many particle-hole  
pairs

**III** decay similar to X-ray edge effect  
double occupancy generates many particle-hole  
pairs

# Kondo energy scale $\Gamma$

$L_f = 120 - 400, m = 128 - 256, \eta = 0.1 - 0.01D$



**Pinning:**  $\rho(0) = \frac{D}{2\pi V^2} \quad \forall U$

$V = D/2, L_f = 120 - 400, m = 256, \eta = 0.1 - 0.05D$

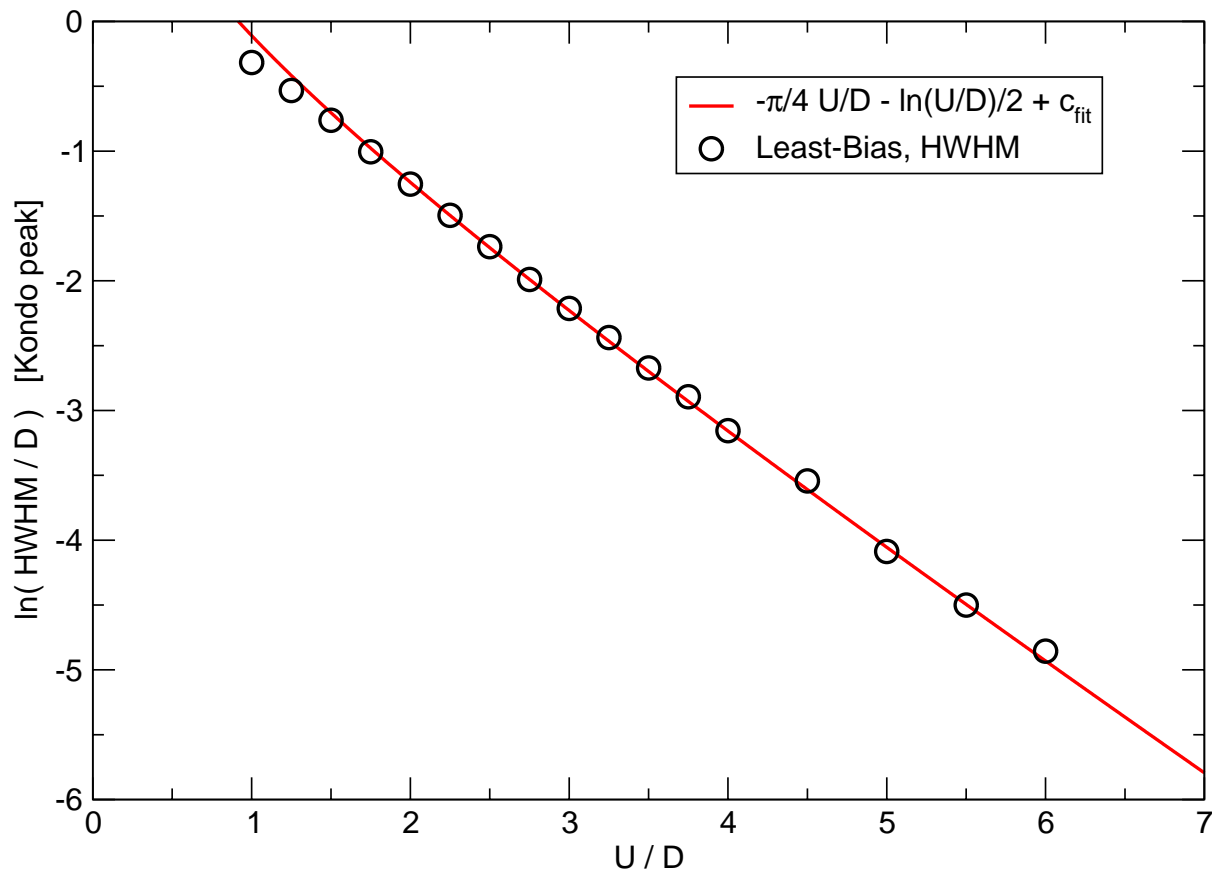
$U/D$	$\pi D\rho(0)$	$U/D$	$\pi D\rho(0)$
1.0	2.00015	3.0	2.00331
1.5	2.00094	3.5	2.00398
2.0	2.00384	4.0	2.00422
2.5	2.00711	5.0	2.04662

# Kondo energy scale II

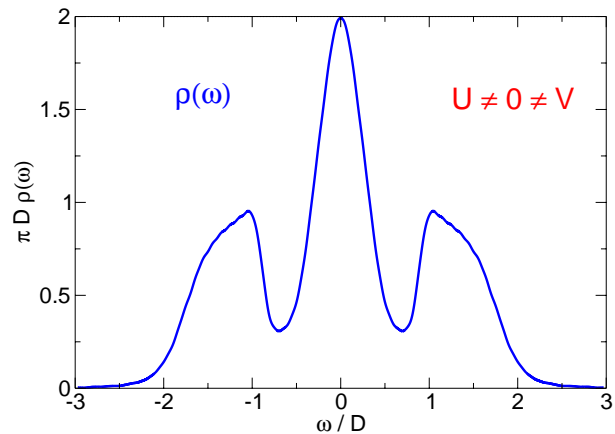
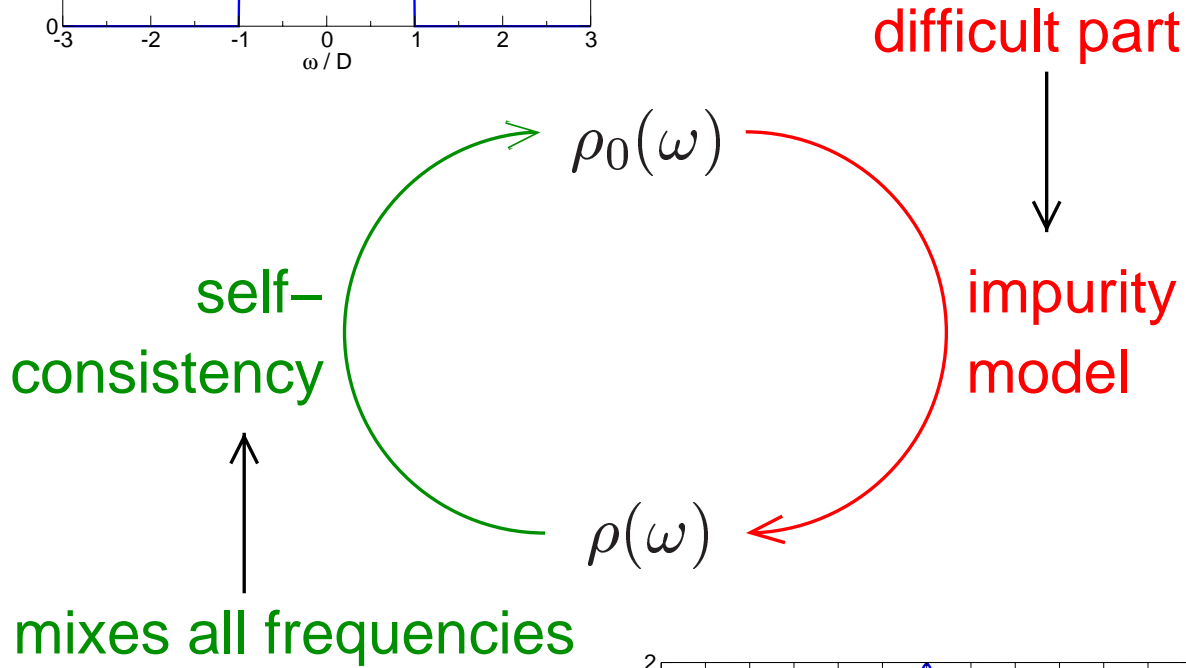
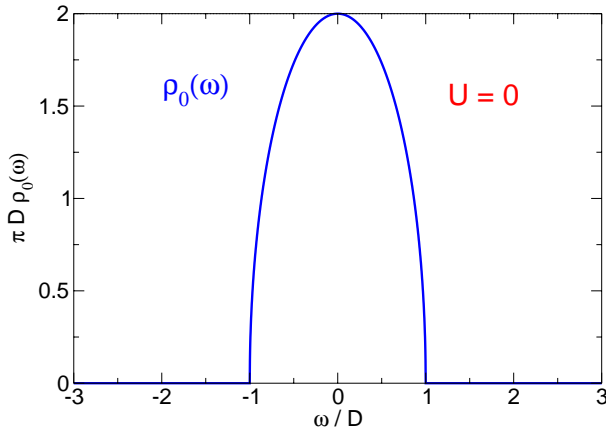
Central peak at  $\omega = 0$ : Abrikosov-Suhl or Kondo resonance

Width set by the exponentially small Kondo scale

$$T_K \propto V \sqrt{\frac{D}{U}} \exp\left(-\frac{\pi U D}{16 V^2}\right) \quad (U > D)$$



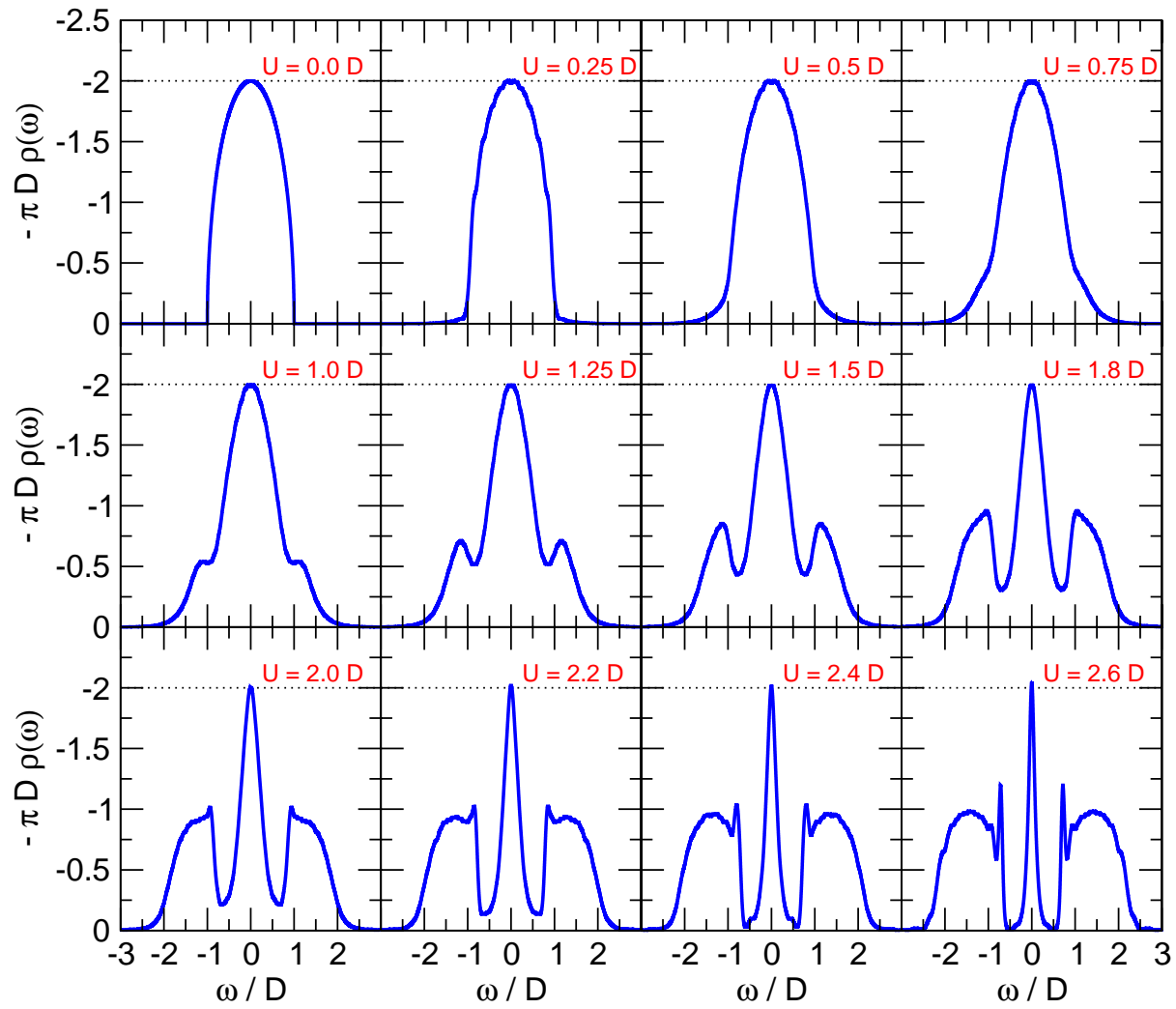
# Dynamical mean field theory (DMFT)



- ▶ lattice models
- ▶  $d = \infty$  (Bethe lattice) Hubbard model

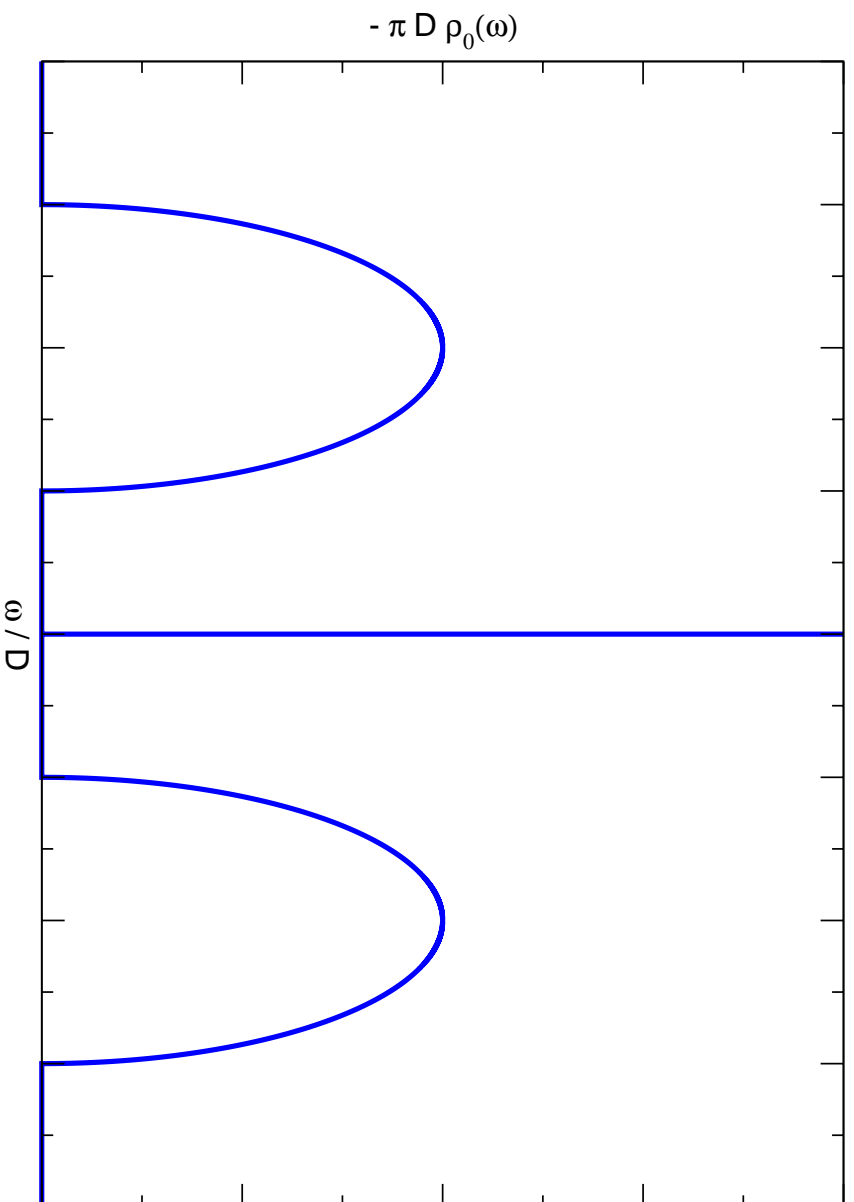
# DMFT: metal

$$L_f = 160, m = 128, \eta = 0.1D$$



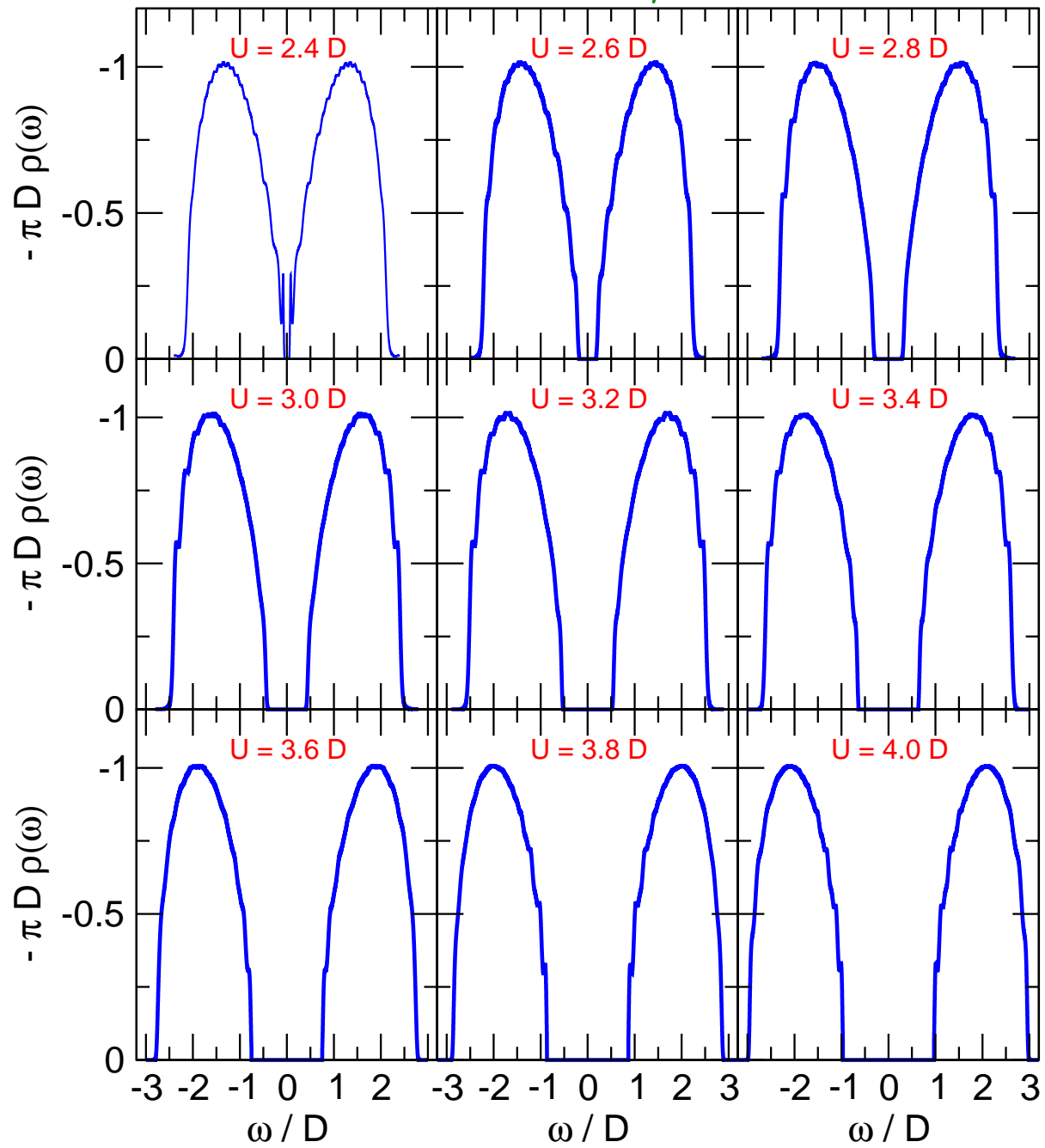
# DMFT: insulator I

- odd number of fermions
- degeneracy in the bath problem: free spin moment
- ▶ must be taken into account by the algorithm
- start DMFT self-consistency cycle from an insulating free bath



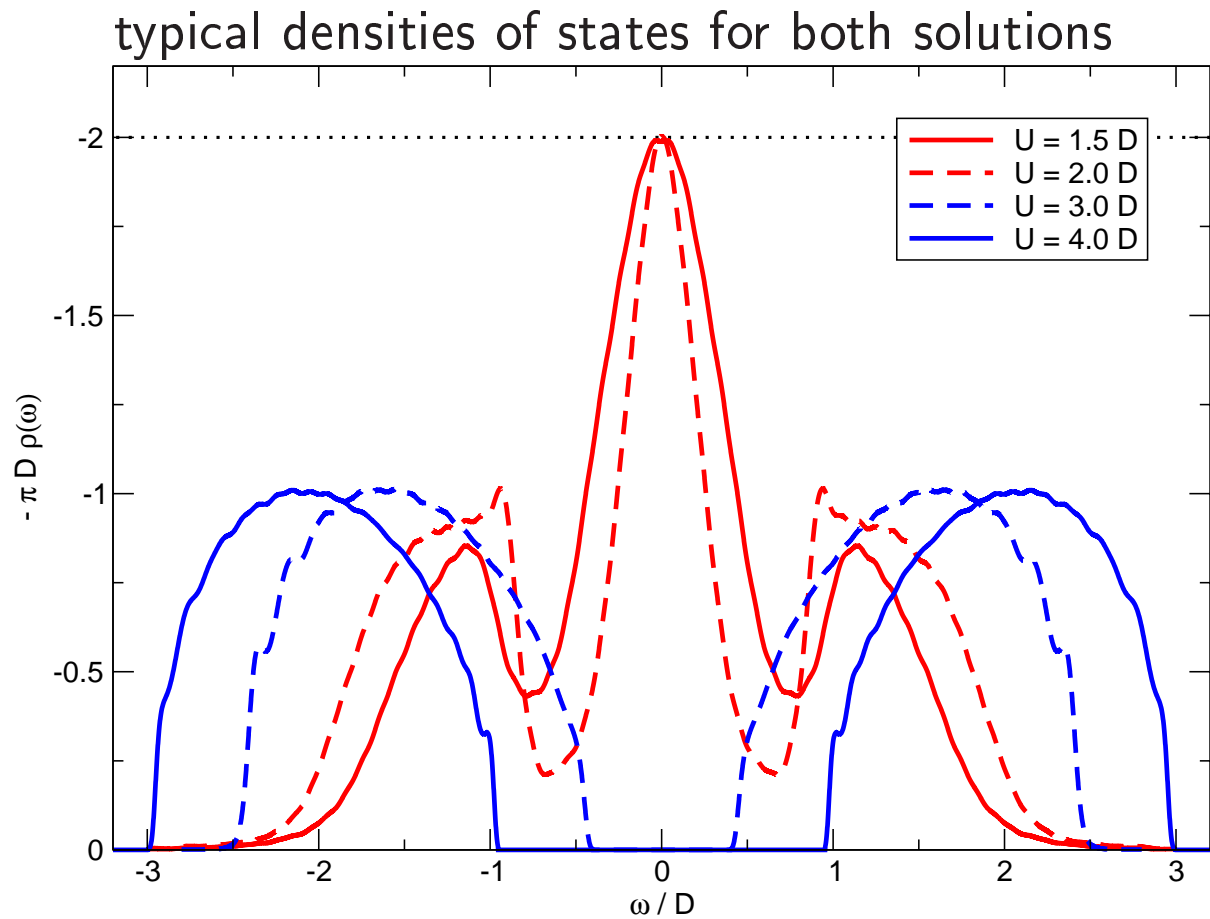
# DMFT: insulator II

$$L_f = 121, m = 128, \eta = 0.1D$$



see also → S. Nishimoto, F. Gebhard, and E. Jeckelmann, [cond-mat/0406666](https://arxiv.org/abs/cond-mat/0406666) (2004)

# DMFT: metal and insulator



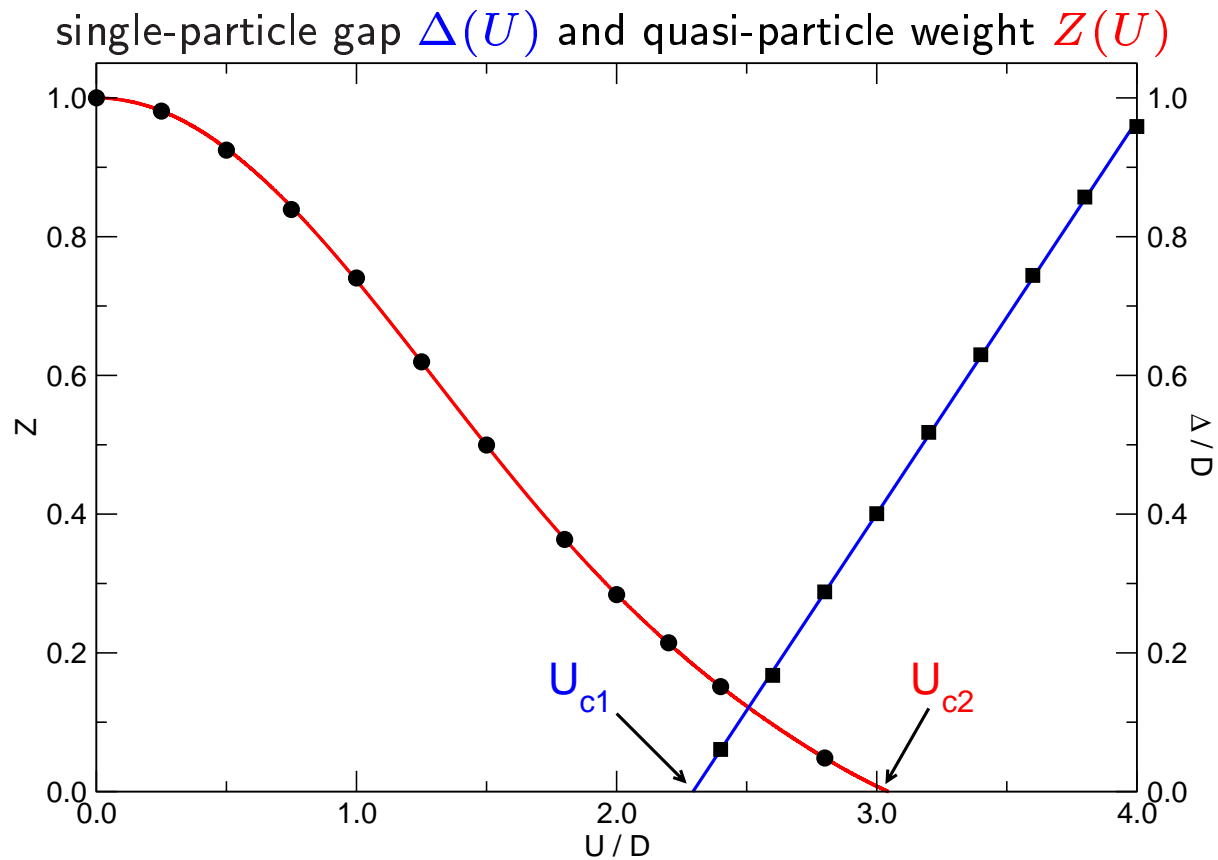
- **no** substructures on the peaks and bands

in contrast to → D.J. García, K. Hallberg, and M.J. Rozenberg,

[cond-mat/0403169](#) (2004)

- **except from:** side peaks on the inner edge of the Hubbard bands in the metallic solution
- ▶ good resolution for all energies

# $U_{c1}$ and $U_{c2}$



authors	method	$U_{c1}/D$	$U_{c2}/D$
Karski <i>et al.</i> (04)	D-DMRG	$2.29 \pm 0.1$	$3.04 \pm 0.1$
Nishimoto <i>et al.</i> (04)	var D-DMRG	$2.225 \pm 0.025$	
García <i>et al.</i> (04)	lan D-DMRG	$2.39 \pm 0.02$	$3.0 \pm 0.2$
Blümer <i>et al.</i> (04)	PT-QMC	2.39	
Bulla <i>et al.</i> (01)	NRG	2.39	2.94
Georges <i>et al.</i> (96)	IPT		3.30

# Summary

- Unbiased algorithm to spectral properties
- Constant/adaptive resolution for all energies
- Novel non-linear positive definite deconvolution scheme: Least-Bias
- Analysis of the lineshape of the Hubbard satellites
- Kondo energy scale reproduced
- Implementation in DMFT self-consistency
  - Good energy resolution also for intermediate and high energies
  - Mott-Hubbard metal-insulator transition

# Outlook

- ▶ Further analysis of the lineshape of the Hubbard satellites
- ▶ Modifications of the model
  - Magnetic fields
  - Away from half-filling
  - More than one orbital
  - Small clusters
- ▶ Implementation in DMFT self-consistency
  - Modified models with self-consistency
  - Description of real strongly correlated materials